Equatorial Pacific productivity and dust flux during the mid-Pleistocene climate transition

Gisela Winckler, Robert F. Anderson,[1] and Peter Schlosser[1,2]

Lamont-Doherty Earth Observatory of Columbia University, Palisades, New York, USA

Received 6 May 2005; revised 30 August 2005; accepted 19 September 2005; published 17 December 2005.

[1] We present a helium isotope record for core TT013-114PC from the central equatorial Pacific (140°W, 4°N, 4432 m water depth) spanning a period of 1 million years. We focus on the time interval from 560 to 800 kyr, largely coinciding with the mid-Pleistocene climate transition (MPT) when the dominant period of the Earth's climate variability shifted from 41 kyr to 100 kyr. The terrigenous ^{4}He concentrations from our study correlate very well with published titanium concentrations in this core strongly supporting the use of terrigenous ^{4}He as a monitor of continental dust. Normalizing titanium and terrigenous ^{4}He concentrations to ^{3}He suggests that the dust supply during the MPT was approximately 30% lower compared to the subsequent period (560–100 kyr). The ^{3}He-normalized barium, aluminum and phosphorus concentrations, trace elements with a predominantly biogenic source in these sediments, are relatively constant. This is in contrast to previous studies that reported an apparent rise of titanium-normalized productivity proxies. Rather than a significant increase in productivity during the MPT, we conclude that the dust flux to the central equatorial Pacific was reduced and that the export productivity was approximately constant during this period of climate reorganization.

Citation: Winckler, G., R. F. Anderson, and P. Schlosser (2005), Equatorial Pacific productivity and dust flux during the mid-Pleistocene climate transition, *Paleoceanography*, *20*, PA4025, doi:10.1029/2005PA001177.

1. Introduction

[2] The most prominent feature of the equatorial Pacific is the upwelling of CO_2-rich subsurface water which creates the largest natural source for the net CO_2 flux from the ocean to the atmosphere [*Takahashi et al.*, 1997, 2002]. The rich nutrients brought up by the upwelling water promote phytoplankton growth, making it one of the major sites of organic carbon export to the deep sea. Export productivity in this region represents a significant part of the global ocean carbon cycle. Thus, the equatorial Pacific has been suggested to have a major influence on global climate via feedbacks involving CO_2 [e.g., *Archer and Maier-Reimer*, 1994; *Broecker and Henderson*, 1998].

[3] One of the key questions in paleoceanography is whether biological productivity in the Pacific has changed substantially during the past. If so, have productivity changes been a direct response to climate forcing and have they provided significant feedbacks through altered air-sea partitioning of CO_2? Modern El Niño events disrupt the natural carbon fluxes and create significant imbalances in the ocean-atmosphere CO_2 exchange [e.g., *Feely et al.*, 1999] highlighting the importance of understanding the role of the ocean carbon cycle in climate change and its sensitivity to climate perturbations. In order to discern the coupling between ocean circulation, productivity and climate, many studies have attempted to estimate past ocean productivity and to develop proxies to reconstruct the history of ocean productivity from marine sediments [e.g., *Bopp et al.*, 2003; *Kohfeld et al.*, 2005].

[4] Another important variable in the global climate system is atmospherically transported mineral aerosols (dust). The concentration of dust in the atmosphere influences the climate system through a variety of processes, e.g., affecting radiative forcing (scattering and absorption of light), condensation processes and by providing nutrients (e.g., iron) to terrestrial and marine biological systems [e.g., *Harrison et al.*, 2001]. A potential factor controlling dust delivery to the equatorial Pacific is the latitudinal position of the Intertropical Convergence Zone [*Rea*, 1994]. Only a few paleorecords of dust deposition in the equatorial Pacific are available. Most of them are limited to the late Pleistocene and show complex and variable patterns. Whether there is a consistent relationship between maximum dust fluxes and interglacial conditions [*Rea*, 1990, 1994] or glacial conditions [*Anderson et al.*, 2005] or no consistent relationship at all [*Murray et al.*, 1995], remains a matter of debate.

[5] The focus of this paper is on reevaluating the export productivity and dust deposition in the equatorial Pacific during the mid-Pleistocene climate transition (MPT). The MPT, i.e., the period when the dominant cyclicity of the Earth's climate evolved from ~41 kyr to ~100 kyr, is thought to represent a period of major climate reorganization [e.g., *Raymo et al.*, 1997]. There is recent evidence for

[1] Also at Department of Earth and Environmental Sciences, Columbia University, New York, New York, USA.

[2] Also at Department of Earth and Environmental Engineering, Columbia University, New York, New York, USA.

0883-8305/05/2005PA001177$12.00

a strong increase in export production in the central equatorial Pacific during the period from 560–800 kyr, broadly coinciding with the MPT [*Murray et al.*, 2000]. Extreme increases in export productivity were found along a transect of cores across the equator at 140°W. The maxima of the export productivity observed during the MPT are much more pronounced than its variability throughout the subsequent glacial/interglacial periods. If this interpretation is correct, then the export productivity in response to the mid-Pleistocene climate transition was greatly enhanced compared to any other time during the late Pleistocene, and represents perhaps the largest biogeochemical response to climate change in the Pacific Ocean during the Pleistocene.

[6] To further investigate the cause of this important feature, we have analyzed ^{3}He and ^{4}He concentrations over the last 1 Myr in core TT013-PC114 in the central equatorial Pacific. This core represents the site along the 140°W transect where the most pronounced relative changes in export productivity were found previously. In equatorial Pacific sediments, ^{3}He is dominated by the extraterrestrial ^{3}He signal from interplanetary dust particles (IDPs) and represents a tool to determine accumulation rates independent from age models [e.g., *Marcantonio et al.*, 1995, 1996, 2001]. We apply this tool to existing records of paleoproductivity (barium, aluminum, phosphorus) and, using existing titanium data and our new ^{4}He record, to reconstruct the dust flux to the central equatorial Pacific. We find relatively constant ratios of the paleoproductivity indicators to ^{3}He throughout the record, and lower Ti/^{3}He and ^{4}He$_{terr}$/^{3}He ratios during the MPT. Rather than an increase in productivity during the MPT, we conclude that there was a reduced flux of mineral aerosols to this region during this period of climate reorganization.

2. Geochemical Background

2.1. Reconstruction of Fluxes

[7] Reconstructing fluxes of sedimentary components is vitally important to many areas of paleoceanographic research. At any particular site, sediment burial rates may be influenced by the rain rate of particulate matter settling through the water column as well as by sediment redistribution. Consequently, strategies have been sought to correct for sediment redistribution and to derive past changes in rain rate unbiased by the influence of sediment focusing.

[8] For sediments deposited during the past 250–300 kyr, normalizing to decay-corrected concentrations of unsupported ^{230}Th (^{230}Th$^0_{ex}$) is the method of choice (for a review see *Francois et al.* [2004]). For older sediments, where the 75 kyr half-life of ^{230}Th precludes its use, there is no consensus concerning the best approach to correct for sediment redistribution.

[9] Some investigators have sought to reconstruct past changes in biological productivity by normalizing trace elements with a predominantly biogenic source (e.g., barium, phosphorus, aluminum) to titanium, the source of which is lithogenic [e.g., *Latimer and Filippelli*, 2002; *Murray et al.*, 2000]. While the elemental ratio approach circumvents the need of accumulation rates for the derivation of fluxes and thus avoids potential complications arising from sediment redistribution, it implicitly relies on the assumption that variability in the supply of titanium has been much less than variability in export production throughout the period of study.

[10] Other investigators have suggested that the flux of interplanetary dust particles (for a review see *Farley* [2001]) to Earth has been relatively uniform in space and time so that the known flux of extraterrestrial ^{3}He contained within interplanetary dust particles (IDPs) (for a review see *Farley* [2001]) can be used to correct for sediment redistribution [e.g., *Marcantonio et al.*, 1995, 1996, 2001; *Winckler et al.*, 2004]. By normalizing to ^{230}Th$^0_{ex}$, the flux of ^{3}He to the Earth has been shown to be constant over the past 250 kyr at a rate of $(0.8 \pm 0.24) \cdot 10^{-12}$ cm^3 STP cm^{-2} kyr^{-1} [*Marcantonio et al.*, 1996, 2001], consistent with estimates from GISP2 and Vostok ice cores ($(0.62 \pm 0.27) \cdot 10^{-12}$ cm^3 STP cm^{-2} kyr^{-1} and $(0.77 \pm 0.25) \cdot 10^{-12}$ cm^3 STP cm^{-2} kyr^{-1}, respectively [*Brook et al.*, 2000]). The flux of IDPs on longer timescales has not been extensively calibrated so far, but efforts to do so by normalizing ^{3}He to ^{10}Be, a constant flux proxy under specific conditions, are underway. In spite of the lack of a dedicated calibration data set, the accretion rate of ^{3}He for the time period of interest to this study (250 kyr to 1 Myr) can be provisionally constrained by using records of ^{3}He [*Patterson and Farley*, 1998] and ^{10}Be (A. Mangini, personal communication, 2005) from core ODP806 in the western equatorial Pacific. Beryllium 10 data have been corrected for radioactive decay and for geomagnetically induced production rate changes following the procedure outlined by *Frank et al.* [2000]. The resulting ^{3}He/^{10}Be$^0_{corr}$ ratios (see Figure 1 and caption) show no trend over the time interval from 250 kyr to 1 Myr with a variability around the mean ^{3}He/^{10}Be$^0_{corr}$ ratio of 23% (1 σ). These findings support the use of extraterrestrial ^{3}He as a constant flux proxy on the Myr timescale.

[11] Using the ^{3}He approach, the accumulation rate of any sedimentary component can be calculated as

$$[F]_{\text{proxy}} = [\text{proxy}] \cdot \text{MAR}_{\text{CF}} = [\text{proxy}] \cdot \frac{f_{^3\text{He}}}{[^3\text{He}]} \quad (1)$$

where MAR_{CF} is the bulk mass accumulation rate derived from the constant flux proxy, [proxy] is the concentration of the component, [^{3}He] is the measured ^{3}He concentration and $f_{^3\text{He}}$ is the constant flux of ^{3}He to the sediments. As shown in equation (1), there is a linear relationship between the proxy/^{3}He ratios and the flux itself, an essential principle that will be used in the discussion of this paper.

2.2. Barium, Aluminum and Phosphorus as Paleoproductivity Proxies

[12] The barium cycle has been shown to be strongly associated with biological activity [e.g., *Bishop*, 1988; *Goldberg and Arrhenius*, 1958; *Paytan et al.*, 1996]. Marine barite ($BaSO_4$) is an authigenic mineral formed within decaying organic matter. It has been shown empirically that its flux is positively correlated with increasing export production [*Dymond et al.*, 1992; *Francois et al.*, 1995]. Excess barium, defined as the fraction of barium not associated with lithogenic material, is frequently used to define barite abundance in sediments and has been extensively used as a proxy to infer paleoproductivity patterns

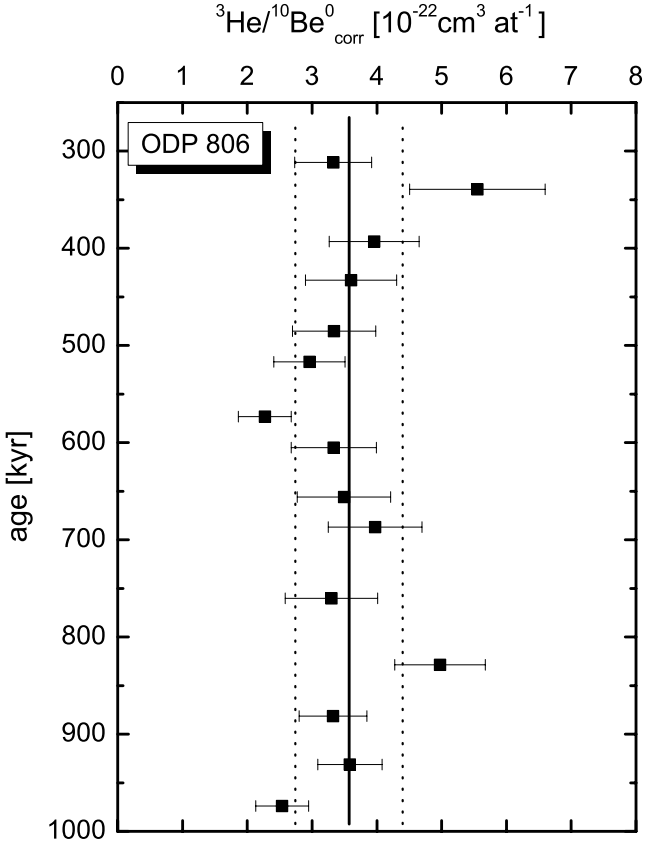

Figure 1. The $^3He/^{10}Be^0_{corr}$ ratios for core ODP806 in the western equatorial Pacific Ocean. ^3He concentrations are from *Patterson and Farley* [1998] and ^{10}Be concentrations are from A. Mangini (personal communication, 2005). The ^3He concentrations were measured using aliquots of homogenized (strip) samples representing 20–30 kyr time intervals, while the ^{10}Be analysis was generated using discrete samples. The ^{10}Be concentrations have been corrected for radioactive decay and for variability in the ^{10}Be production due to variable strength of the magnetic field of the Earth after *Masarik and Beer* [1999]. The intensity of the magnetic field was reconstructed for the past 800 kyr after *Guyodo and Valet* [1999] and was reconstructed for the time period before 800 kyr after *Valet and Meynadier* [1993]. To compensate for the different resolution of both records, $^3He/^{10}Be^0_{corr}$ ratios were determined at the depth of the ^{10}Be sample by dividing the ^3He concentration in the composite sample spanning the depth of the discrete beryllium analysis by the respective $^{10}Be^0_{corr}$ concentration. The straight line gives the mean of the $^3He/^{10}Be^0_{corr}$ ratio; the dotted lines indicate the standard deviation of the mean.

[e.g., *Dean et al.*, 1997; *Francois et al.*, 1995; *Nürnberg et al.*, 1997; *Schwarz et al.*, 1996].

[13] Studies in the equatorial Pacific have documented that significant amounts of aluminum are contained both in lithogenic phases and authigenic phases [e.g., *Dymond et al.*, 1997; *Murray and Leinen*, 1996; *Murray et al.*, 1993]. For these sediments, scavenged excess aluminum, the component of aluminum that is unsupported by the lithogenic fraction, has been found to reflect the bulk biogenic particle flux through the water column and to the seafloor and is therefore used as paleoproductivity proxy [*Banakar et al.*, 1998; *Dymond et al.*, 1997; *Murray and Leinen*, 1996; *Murray et al.*, 1993, 2000].

[14] Similarly, the use of phosphorus as paleoproductivity proxy is based on observed correlations between the phosphorus distribution in sediments and biogenic fluxes through the water column to the seafloor [e.g., *Delaney*, 1998; *Froelich et al.*, 1982; *Latimer and Filippelli*, 2002].

2.3. Terrigenous ^4He as Dust Proxy

[15] Terrigenous ^4He has been introduced as a proxy of dust in marine sediments by *Patterson et al.* [1999]. As old continental material contains high radiogenic ^4He concentrations (e.g., $2000 \cdot 10^{-9}$ $cm^3 \cdot g^{-1}$ in Asian dust [*Farley*, 1995]) compared to relatively low ^4He contents in other terrigenous components (e.g., $5 \cdot 10^{-9}$ $cm^3 \cdot g^{-1}$ in volcanic ashes [*Patterson et al.*, 1999]), the terrigenous ^4He signal tracks old continental dust and is not affected by other terrigenous components. Helium does not exist as organic complex, nor is it incorporated into biogenic phases; therefore terrigenous ^4He can be assumed to be entirely contained within detrital material.

3. Samples and Methods

[16] Samples were analyzed from piston core TT013-PC114 (4.04°N, 139.85°W, 4432 m water depth) collected in the framework of the JGOFS (Joint Global Ocean Flux Study) program. The age model was determined by correlating the $CaCO_3$ concentration profile in PC114 to the $CaCO_3$ records of nearby cores with $\delta^{18}O$ constrained age models (cores TT013-PC18 at 2°S and TT013-PC72 at the equator, both along 140°W [*Knowlton*, 1998; *Murray et al.*, 2000]).

[17] Helium isotopes were measured on samples taken between 20 cm and 775 cm core depth, a section that represents a time interval of about 935 kyr. Individual sediment sample aliquots of 1.5 to 2.5 g were leached in 200 mL of 0.5 N acetic acid to remove carbonate material which carries no substantial amount of helium and were then washed three times in distilled water. This resulted in residues of about 200 mg which were wrapped in aluminum foil and placed in the furnace of the gas inlet system. Helium was extracted from the samples at ~1300°–1400°C. During extraction the furnace was kept exposed to a liquid nitrogen cooled charcoal trap in order to remove CO_2, H_2O and organic compounds. Further purification was performed by exposure to a SAES getter at room temperature. The gas was then collected on a cryogenically cooled charcoal trap held at ~13 K and helium was separated from neon by heating the trap to 45 K. Abundance and isotopic analyses were performed with a MAP215-50 noble gas mass spectrometer calibrated with a known volume of a Yellowstone helium standard (MM) with a $^3He/^4He$ ratio of 16.45 R_a (where $R_a = (^3He/^4He)_{air} = 1.384 \cdot 10^{-6}$ [*Clarke et al.*, 1976]). Typical hot blanks were $1–2 \cdot 10^{-10}$ cm^3 STP ^4He with approximately atmospheric $^3He/^4He$ ratios, and represent small corrections (<1%) to the samples. The

Table 1. Helium Isotope Data of TT013-PC114[a]

Depth, cm	Age, kyr	^{3}He, 10^{-12} cm^3 STP g^{-1}	^{3}He/^{4}He (R/R_a)	^{4}He$_{terr}$, 10^{-8} cm^3 STP g^{-1}
20[b]	15	1.422 ± 0.028	32.2 ± 0.5	2.604 ± 0.051
40	30	1.227 ± 0.026	35.3 ± 0.6	2.001 ± 0.042
60	46	1.183 ± 0.024	37.9 ± 0.6	1.764 ± 0.036
80[b]	60	1.7215 ± 0.034	30.0 ± 0.5	3.420 ± 0.069
120[b]	113	5.843 ± 0.117	33.6 ± 0.6	10.11 ± 0.21
140	145	1.392 ± 0.028	27.0 ± 0.4	3.145 ± 0.061
150	153	1.529 ± 0.032	26.4 ± 0.5	3.542 ± 0.075
165	164	2.997 ± 0.060	35.7 ± 0.6	4.822 ± 0.094
185[b]	179	8.855 ± 0.186	27.3 ± 0.4	19.691 ± 0.382
200[b]	219	4.385 ± 0.088	29.2 ± 0.5	9.034 ± 0.183
215	259	2.084 ± 0.040	43.1 ± 0.7	2.623 ± 0.051
225	265	3.209 ± 0.064	27.0 ± 0.4	7.264 ± 0.141
235[b]	271	6.399 ± 0.128	25.8 ± 0.5	15.271 ± 0.322
275	334	1.805 ± 0.036	28.9 ± 0.5	3.756 ± 0.076
290[b]	358	5.865 ± 0.117	33.5 ± 0.6	10.226 ± 0.207
310	388	9.047 ± 0.181	39.2 ± 0.6	12.890 ± 0.250
325	400	2.212 ± 0.044	40.6 ± 0.7	3.012 ± 0.061
350	452	1.444 ± 0.030	29.1 ± 0.5	2.982 ± 0.060
380[b]	481	8.788 ± 0.176	46.3 ± 0.7	10.060 ± 0.195
415	525	1.551 ± 0.033	34.9 ± 0.6	2.561 ± 0.054
435	564	3.875 ± 0.078	31.9 ± 0.5	7.152 ± 0.145
460[b]	583	2.933 ± 0.062	39.3 ± 0.7	4.158 ± 0.084
485	637	0.999 ± 0.020	43.0 ± 0.7	1.264 ± 0.025
500	659	0.698 ± 0.017	43.7 ± 1.0	0.863 ± 0.022
510	672	1.191 ± 0.024	70.4 ± 1.1	0.725 ± 0.014
525	677	0.994 ± 0.023	33.6 ± 0.7	1.720 ± 0.039
555[b]	687	4.429 ± 0.097	41.7 ± 0.8	5.811 ± 0.128
580[b]	710	0.953 ± 0.019	41.1 ± 0.7	1.277 ± 0.026
595	724	1.333 ± 0.027	48.8 ± 0.8	1.418 ± 0.028
605	736	0.869 ± 0.018	47.3 ± 0.9	0.966 ± 0.021
630[b]	766	1.637 ± 0.033	37.3 ± 0.6	2.493 ± 0.050
655[b]	795	3.671 ± 0.081	41.4 ± 0.8	4.916 ± 0.108
690[b]	837	4.912 ± 0.098	38.4 ± 0.7	7.100 ± 0.144
745	907	4.794 ± 0.096	41.4 ± 0.7	6.370 ± 0.124
775[b]	935	3.194 ± 0.064	30.3 ± 0.6	6.278 ± 0.143

[a]Helium concentrations are reported in units of cm^3 STP per gram of sediment. The ^{3}He/^{4}He ratios are normalized to the atmospheric ratio (R_a = 1.384 × 10^{-6} [*Clarke et al.*, 1976]. Here ^{4}He$_{terr}$ represents the terrigenous fraction of ^{4}He (see sections 2.3 and 4.2). Quoted errors are the analytical uncertainties of the mass spectrometric analysis.

[b]Marked samples were duplicated; in these cases, average values are reported.

analytical precision of the mass spectrometric analysis is on the order of 1% for ^{4}He and 2–3% for ^{3}He. Note that the natural variability in the ^{3}He concentration of a sample is controlled by the statistical effect of the small number of IDPs hosted in the sediments and is a greater source of uncertainty than the analytical precision. Replicates were run for samples as indicated in Table 1, and the reproducibility distribution is in good agreement with the model prediction of *Farley et al.* [1997]. Following *Farley et al.* [1997] and *Patterson and Farley* [1998], the 1 σ uncertainty is therefore estimated to be ∼20% for a single and ∼15% for a duplicate analysis, respectively.

4. Results and Discussion

4.1. The ^{3}He record

[18] The observed ^{3}He/^{4}He ratio (see Table 1 for results) reflects the mixing of extraterrestrial and terrigenous material. Assuming typical ^{3}He/^{4}He ratios for these end-members, 2 · 10^{-8} for terrigenous helium [*Ozima and Podosek*, 1983] and 2.4 · 10^{-4} for extraterrestrial helium [*Nier and Schlutter*, 1992], the amount of IDP-derived ^{3}He in the sediments can be estimated from the observed ^{3}He/^{4}He ratio using a simple two component mixing model

$$\frac{^3\mathrm{He}_{\mathrm{IDP}}}{^3\mathrm{He}_{\mathrm{meas}}} = \left(\frac{1 - \frac{(^3\mathrm{He}/^4\mathrm{He})_{\mathrm{terr}}}{(^3\mathrm{He}/^4\mathrm{He})_{\mathrm{meas}}}}{1 - \frac{(^3\mathrm{He}/^4\mathrm{He})_{\mathrm{terr}}}{(^3\mathrm{He}/^4\mathrm{He})_{\mathrm{ET}}}} \right) \quad (2)$$

where "ET" denotes the extraterrestrial and "terr" denotes the terrigenous component. Following this approach, it was determined that the non-IDP component of the ^{3}He measured in our samples is negligible throughout the core. The lowest proportion of IDP-derived ^{3}He (reflected by the lowest ^{3}He/^{4}He ratio) is found in a sample at 235cm (271 kyr) where it still contributes 99.95% of the total ^{3}He concentration. Therefore we use the total ^{3}He concentration as approximation for extraterrestrial ^{3}He.

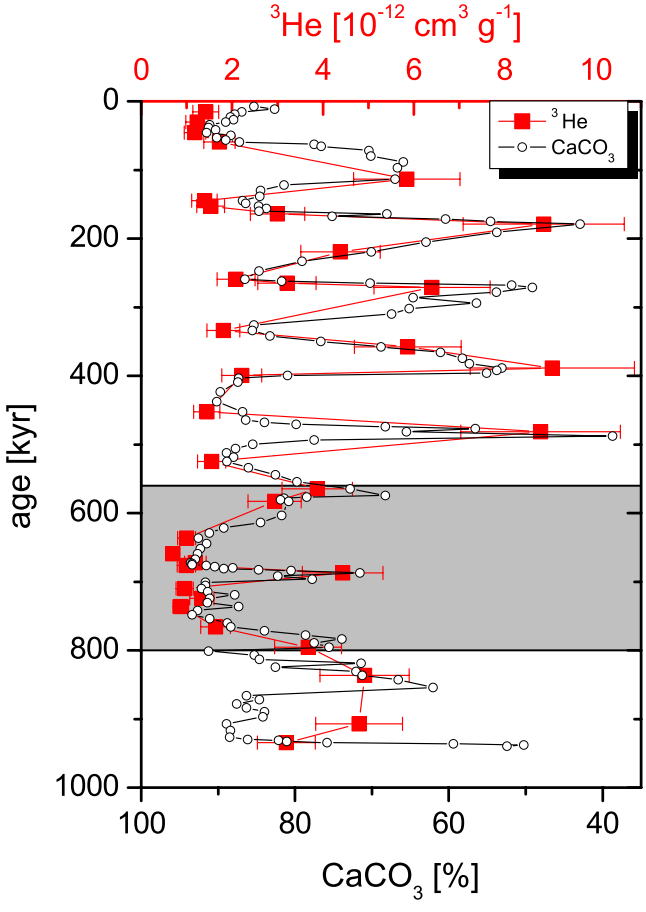

Figure 2. Down-core profiles of the ^{3}He concentration and calcium carbonate content (on a reverse scale to orient the peaks with the ^{3}He record) plotted against age of sediments for core PC114. Shaded region represents the time period between 560 and 800 kyr, identified as representing the mid-Pleistocene climate transition by *Murray et al.* [2000].

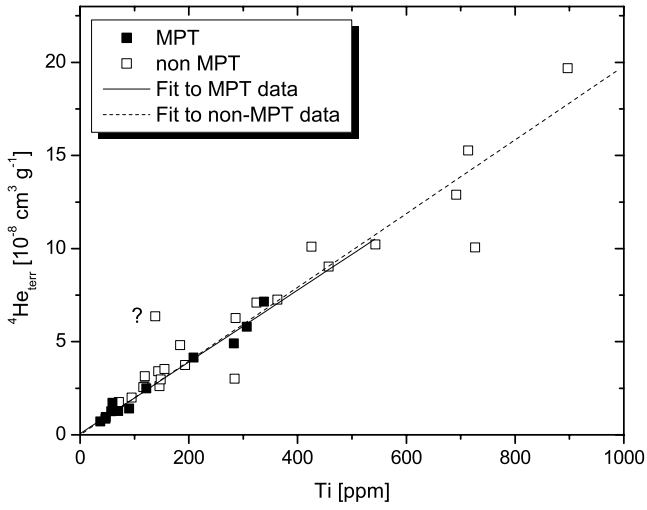

Figure 3. Property-property plot of the terrigenous fraction of ^{4}He, calculated as defined in the text, versus titanium concentration for core PC114. Solid squares represent samples from the MPT; open squares represent samples from before and after the MPT. The solid line is a linear regression to the data from the MPT; the dashed line is a fit to the data representing the pre- and post-MPT period. The correlation factors for the linear fits are 0.98 and 0.95, respectively.

[19] Depth profiles of the ^{3}He concentration and the $CaCO_3$ content are shown in Figure 2. Carbonate data as well as barium, aluminum, phosphorous, and titanium data are from *Murray et al.* [2000] and have been retrieved from World Data Center for Paleoceanography (http://www.ncdc.noaa.gov/paleo/index.html).

[20] The most prominent feature of the carbonate record is the pattern of cyclic and high-amplitude fluctuations of $CaCO_3$ preservation with depth as has been described by previous investigators [*Arrhenius*, 1952; *Farrell and Prell*, 1989]. The $CaCO_3$ preservation record exhibits a strong periodicity at about 100 kyr and is generally described by good preservation during glacial stages and poor preservation during interglacials.

[21] Helium 3 concentrations vary between 0.7 and $9 \cdot 10^{-12}$ cm^3 STP g^{-1}. The correlation between ^{3}He concentration and carbonate content throughout the glacial/interglacial stages back to MIS20 is very good (Figure 2). The ^{3}He profile apparently reflects variable dilution of the constant ^{3}He input from IDPs by $CaCO_3$, the principal component of these sediments. The only sample that does not follow the tight correlation is that at 907 kyr for which the ^{3}He concentration seems to be anomalously high. As there is no analytical reason to discard the measurement and a replicate sample was not available for analysis we decided to keep this value in the data set and flag it ("?") in Figures 3–5.

4.2. The ^{4}He Record

[22] Helium 4 concentrations range from 10 to $230 \cdot 10^{-9}$ cm^3 STP g^{-1}. In contrast to ^{3}He, the ^{4}He signal in the sediment is dominated by the terrigenous component. Using a simple two-component mixing model

$$\frac{^4He_{terr}}{^4He_{meas}} = \frac{(^3He/^4He)_{meas} - (^3He/^4He)_{ET}}{(^3He/^4He)_{terr} - (^3He/^4He)_{ET}} \quad (3)$$

the amount of terrigenous ^{4}He was determined (Table 1). The relative contribution of terrigenous ^{4}He ($^4He_{terr}$) to total ^{4}He component ranges from 60 to 85%. The correlation between titanium and $^4He_{terr}$ concentrations at PC114 is excellent (Figure 3) and supports the application of $^4He_{terr}$ as monitor of continental dust. The strong correlation between the two proxies is inconsistent with the interpretation of *Kryc et al.* [2003] who recently challenged the traditional view that titanium is predominantly supplied by dust and argued that up to 80% of the titanium in biogenic sediments from the central equatorial Pacific occurs as organic complexes. Because terrigenous ^{4}He does not build organic complexes, we would expect significant variability around the mean relationship between titanium and $^4He_{terr}$ if, in fact, a large and variable fraction of the titanium in PC114 sediments occurred as organic complexes. Contrary to this expectation, the good correlation between $^4He_{terr}$ and titanium indicates the absence of a large and variable nondetrital component of titanium. Titanium, like $^4He_{terr}$, appears to be contained predominantly within detrital mineral phases and track the dust input to equatorial Pacific sediments.

4.3. Reevaluation of the Export Productivity Record During the Mid-Pleistocene Climate Transition

[23] Figure 4 compares the barium, aluminum and phosphorus data normalized to extraterrestrial ^{3}He to the same proxy data normalized to titanium as originally presented by *Murray et al.* [2000]. The most prominent feature of the titanium-normalized records are pronounced maxima of the elemental ratios (Ba/Ti, Al/Ti, P/Ti) during the MPT which have been interpreted as indication for a strong increase in export production [*Murray et al.*, 2000]. Normalizing to ^{3}He eliminates the apparent peaks observed in the titanium-normalized barium, aluminum and phosphorus records during the MPT. Whereas the Ba/^{3}He and P/^{3}He ratios are relatively constant throughout the record, the Al/^{3}He ratio even seems to show slightly lower values during the MPT (see discussion below).

[24] The ^{3}He data allow us to discriminate between increased export production (increase of numerator) and reduced titanium flux (decrease of denominator) as the principal cause for increased element/Ti ratios. The long-term trend of the Ti/^{3}He record (Figure 5b) is complementary to the trend in the Ba/Ti ratios (Figure 5a) shown as an example of the records in Figure 4. In particular, the ^{3}He-normalized titanium values are significantly lower during the MPT than during the post-MPT period. This implies that the supply of titanium at this site was significantly lower during the MPT than during the subsequent glacial/interglacial cycles and that the maxima of the element ratios (Ba/Ti, Al/Ti, P/Ti) during the MPT is due to reduced titanium supply, rather than due to increased biological productivity. Thus, on the basis of the ^{3}He-normalized

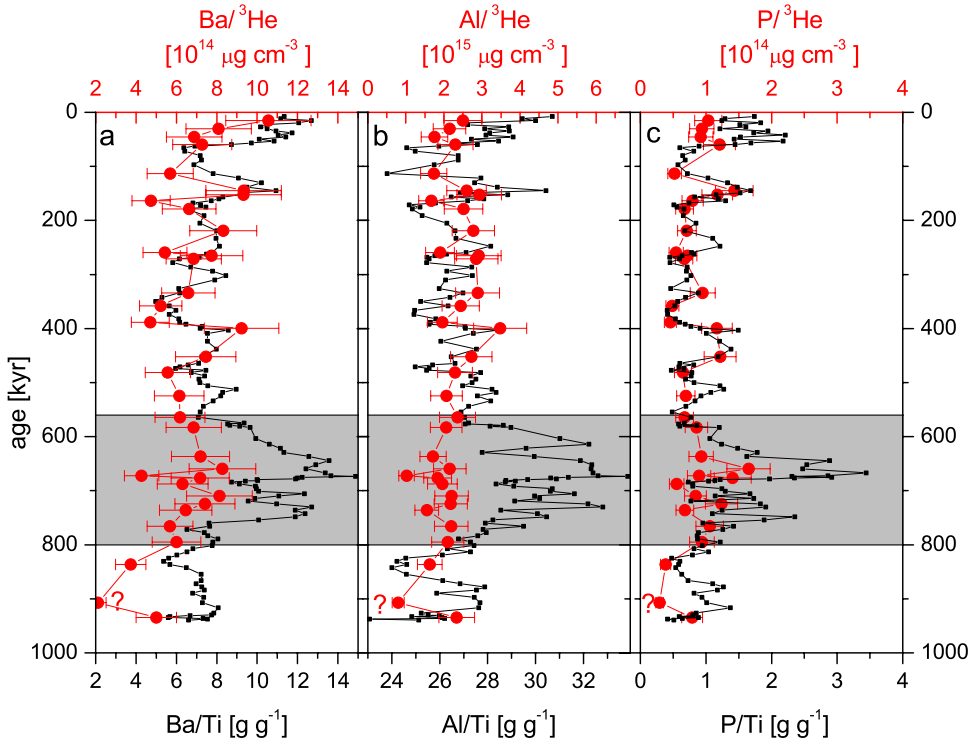

Figure 4. Comparison of the down-core profiles of (a) barium, (b) aluminum, and (c) phosphorus, normalized to titanium (black) and to ^{3}He (red). Shaded region represents the time period between 560 and 800 kyr, representing the mid-Pleistocene climate transition.

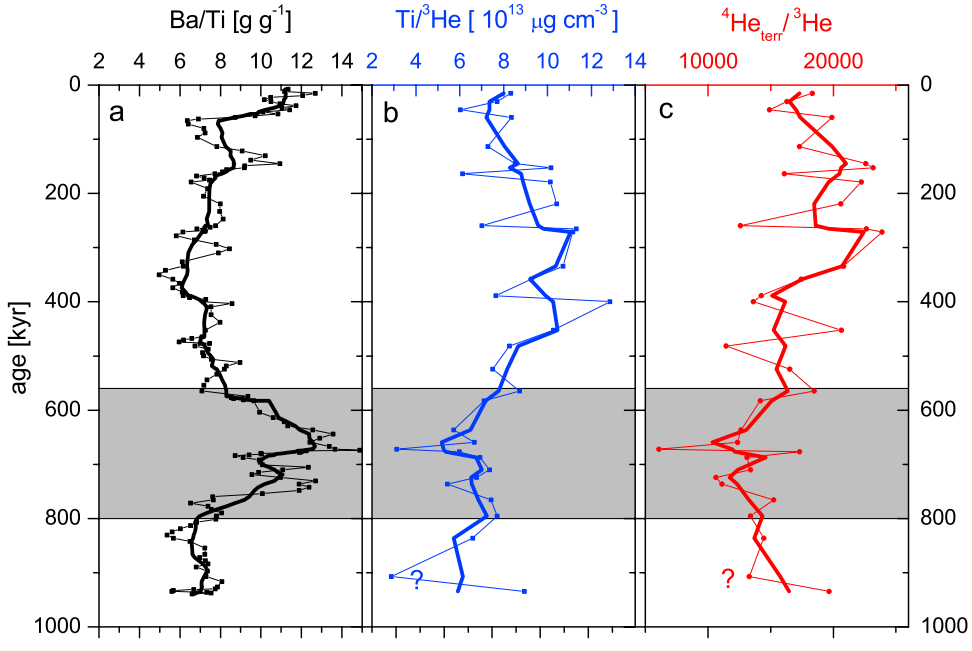

Figure 5. Comparison of down-core profile of the (a) Ba/Ti ratios with the (b) ^{3}He-normalized titanium and (c) ^{3}He-normalized ^{4}He$_{terr}$ record. The bold lines indicate the long-term trend and represent running averages over ~80 kyr. This corresponds to 13-point running averages in the case of Ba/Ti and 3-point running averages in the case of the ^{3}He-normalized values in order to compensate for the different time resolution of both records (^{3}He, mean resolution ~25 kyr; Ba, mean resolution 6 kyr). Shaded region represents the time period between 560 and 800 kyr, representing the mid-Pleistocene climate transition.

Table 2. Mean Element Ratios for MPT and Post-MPT[a]

	Post-MPT	MPT	$\Delta_{MPT/PostMPT}$
Ti/^{3}He, 10^{13} μg cm^{-3}	9.3 ± 0.9	6.5 ± 0.8	0.70
Ba/Ti, g g^{-1}	7.3 ± 0.7	10.3 ± 1.44	1.4
^{4}He$_{terr}$/^{3}He	18580 ± 2350	13130 ± 1690	0.71
Al/^{3}He, 10^{15} μg cm^{-3}	2.5 ± 0.2	1.92 ± 0.19	0.77

[a]Mid-Pleistocene climate transition (MPT) is 560–800 kyr as defined by *Murray et al.* [2000]. Post-MPT is 100–560 kyr. The time period 560–100 kyr was selected to represent the "plateaus" both in Ti/^{3}He and Ba/Ti ratios in the period following the MPT without including the drop in titanium supply and strong increase in Ba/Ti ratios toward the present. The choice of the upper limit, 100 kyr, is somewhat arbitrary; however, sensitivity tests show that the conclusions do not depend on the exact choice of the upper limit. Mean ratios were calculated for the long-term trend of the data in order to eliminate the high glacial/interglacial variability in the time period 560–100 kyr. Quoted errors are standard deviations of the mean ratios.

records (Figure 4) we infer that productivity during the climate reorganization of the MPT was comparable to the productivity levels in the late Pleistocene.

4.4. Dust Input During the Mid-Pleistocene Climate Transition

[25] In the central equatorial Pacific, the predominant source of titanium is aeolian dust [e.g., *Chuey et al.*, 1987; *Murray and Leinen*, 1993]. The drop in titanium supply during the MPT could reflect either a substantially reduced dust input to this site or, alternatively, a major change in dust provenance, from a dust source with higher titanium concentrations to a dust source low in titanium.

[26] The good correlation between ^{4}He$_{terr}$ and titanium argues against a significant change in provenance. As shown in Figure 3, the correlation between the two proxies is almost identical for the samples during the MPT and before and after. A change in provenance of the dust, without an accompanying change in the Ti/^{4}He$_{terr}$ ratio of the source region, appears to be highly unlikely. Therefore we conclude that the drop in titanium supply reflects a reduced dust input during the MPT compared to late Pleistocene levels. Because the supply of dust to the ocean surface is affected by climate and is potentially variable in time [e.g., *Harrison et al.*, 2001; *Kohfeld and Harrison*, 2001], a significant change in dust flux appears to be a likely response to a major climate reorganization.

[27] Latitudinal variations in the position of the Intertropical Convergence Zone (ITCZ) represent a potential control on the dust delivery to the equatorial Pacific [*Rea*, 1994]. Given the proximity of core PC114 (4°N) to the modern position of the ITCZ, it is an important question whether the variability of the titanium flux recorded at PC114 could have been influenced by a meridional shift in the mean position of the ITCZ or is rather representative of changes in the dust supply to the entire central equatorial Pacific. Evidence against a significant influence by an ITCZ shift comes from the study of *Murray et al.* [2000] who reported alike patterns of variability of Ba/Ti profiles at station PC114 and station PC32 at 5°S along the meridional transect at 140°W, particularly a similar amplitude of the strong MPT maximum. If there was a shift in the position of the ITCZ during the MPT, we would expect the Ba/Ti ratios at PC114 to be more affected than those at PC32 at 5°S. On the basis of the similarity between the Ba/Ti records at 4°N and 5°S we therefore conclude that the drop in titanium supply recorded at PC114 most likely represents a reduction in dust supply throughout the region during the MPT rather than a relocation of the ITCZ.

4.5. Quantifying the Variability of the Dust Input

[28] The long-term trend of the dust flux, as inferred from the ^{4}He$_{terr}$/^{3}He ratios (Figure 5c), shows the same basic features as the Ti/^{3}He record (Figure 5b). Following the relatively low dust input levels during the MPT, there is an increase to higher values in the period 550–250 kyr and a subsequent decrease during the past ~250 kyr to values comparable to the MPT. While the Ti/^{3}He ratios are relatively stable during the MPT, there is considerable variability in the ratios during the period since 560 kyr.

[29] We quantitatively evaluated the extent to which dust fluxes increased following the MPT by comparing the mean values for the MPT time slice and the subsequent period (560–100 kyr, Table 2). The mean Ti/^{3}He ratio during the MPT is about 70% of the Ti/^{3}He ratio during the post MPT period, indistinguishable from the corresponding changes in the ^{4}He$_{terr}$/^{3}He ratio. Both independent dust proxies, titanium and ^{4}He$_{terr}$, indicate a consistent reduction of ~30% in aeolian dust flux to this site during the mid-Pleistocene climate reorganization compared to average late Pleistocene levels.

[30] The information in Table 2 can also be used to check if the reduced dust level can quantitatively explain the apparent productivity peak. Scaling the Ba/Ti ratio of the post-MPT period with this reduced titanium supply yields

$$\left(\frac{\mathrm{Ba}}{\mathrm{Ti}}\right)_{\mathrm{MPT}} = \frac{\left(\frac{\mathrm{Ba}}{\mathrm{Ti}}\right)_{\text{Post-MPT}}}{\Delta_{\mathrm{Ti}}} = \frac{7.3}{0.7} = 10.4 \qquad (4)$$

and matches well the observed value (10.3, Table 2). Accordingly, the 30% decrease of the titanium supply fully accounts for the observed mean increase of the Ba/Ti ratio during the MPT without invoking any change of the barium flux, and thus paleoproductivity.

4.6. Cross-Check With Aluminum Data

[31] The ^{3}He-normalized aluminum record (Figure 4b) provides a sensitive internal consistency check of the hypothesis of a reduced dust flux during the MPT. Particularly, it provides an independent approach to evaluate whether reduced dust flux or an increased IDP and thus ^{3}He flux is responsible for the patterns shown in Figure 5. Since only part of the total aluminum is contained in dust (section 2.2), its flux should be less affected by a reduced dust input than that of the "pure" dust tracers. Accordingly, if the flux of mineral aerosols were lower during the MPT, then we would expect the amplitude of the change in Al/^{3}He to be less than that for Ti/^{3}He or ^{4}He$_{terr}$/^{3}He, respectively. On the other hand, if the flux of IDPs was greater during the MPT (and responsible for the features of Figure 4), then we would expect the MPT reductions in Al/^{3}He, Ti/^{3}He and ^{4}He$_{terr}$/^{3}He to be of similar amplitude. We observe a Al/^{3}He reduction that is smaller, 23%versus ~30% from Ti/^{3}He and ^{4}He$_{terr}$/^{3}He (Table 2), consistent with the observation of

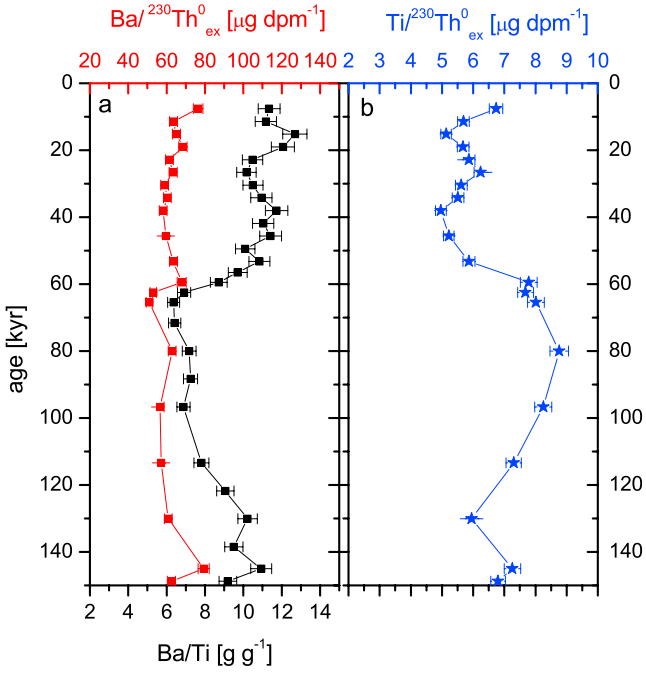

Figure 6. (a) Comparison of the down-core profile of barium, normalized to titanium (black) and $^{230}Th^{0}_{ex}$ (red). (b) The $^{230}Th^{0}_{ex}$-normalized titanium record for the past 150 kyr. (Thorium data are available from US JGOFS database at http://usjgofs.whoi.edu.)

slightly higher (by about 12%) Al/Ti ratios during the MPT. This observation strongly supports the view that the flux of IDPs remained relatively constant while the flux of dust was diminished during the MPT.

4.7. Glacial/Interglacial Variability

[32] Apart from the long-term trend discussed so far, the dust and productivity records show considerable variability on shorter timescales. However, owing to the limited resolution of the post-MPT ^{3}He record the pattern of the late Pleistocene glacial/interglacial cycles cannot be resolved.

[33] A high-resolution $^{230}Th^{0}_{ex}$ record is available for PC114 for the past 150 kyr [*Anderson et al.*, 2005] (raw data archived in the U.S. JGOFS database, http://usjgofs.whoi.edu) and can be used to evaluate the variability of the productivity and the dust signal on a glacial-interglacial timescale. As an example, the Ba/Ti ratios show significant variability over the past 150 kyr (Figure 6a), including a strong increase at about 65 kyr to relatively high values during the past 50 kyr. When the barium concentrations are normalized to $^{230}Th^{0}_{ex}$, the variability is eliminated, and the Ba/$^{230}Th^{0}_{ex}$ ratios are relatively constant over the past 150 kyr. The Ti/$^{230}Th^{0}_{ex}$ record is complementary to the Ba/Ti values indicating that the temporal variability of the Ba/Ti ratios is dominated by changes in the dust (Ti) supply and is not due to changes in export production. The $^{230}Th^{0}_{ex}$-based results are analogous to our observations for the long-term trend, based on the ^{3}He normalization, in showing that the variability of Ba/Ti ratios reflects changes in the supply of titanium rather than changes in the flux of barium. Productivity at this location has been relatively constant over the last glacial cycle, as it was through the MPT.

5. Conclusions

[34] Reconstruction of paleofluxes on longer timescales provides a challenge to paleoceanography. Extraterrestrial ^{3}He is shown to be a valuable tool to normalize fluxes on a Myr timescale. Our study also confirms terrigenous ^{4}He as a reliable tracer of continental dust in the sedimentary record that provides independent and complementary information to other dust proxies such as titanium.

[35] Normalizing titanium and terrigenous ^{4}He to ^{3}He reveals dust fluxes to the central equatorial Pacific during the MPT that were lower by approximately 30% compared to the subsequent time period. Relatively constant Ti/$^{4}He_{terr}$ ratios rule out a change in provenance of the dust to be responsible for the reduced titanium supply during the MPT.

[36] The ^{3}He normalization of barium, aluminum, and phosphorus implies that export productivity was relatively constant throughout the entire record. In particular, the mid-Pleistocene climate transition does not appear to be characterized by elevated productivity levels. This implies that the increase in dust levels from the MPT to the post-MPT phase did not have a significant impact on the export productivity.

[37] Our record implies that mean dust levels recorded in the central equatorial Pacific core site were higher during the late Pleistocene (<560 kyr) than during the previous period (>560 kyr). If this trend was extrapolated toward the early Pleistocene, then it would imply that the 100 kyr world was on average dustier than the 41 kyr world, consistent with the change in amplitude of the global ice volume. Alternatively, if the dust levels were higher during the period before ~900 kyr one could speculate about modulation of the dust input with a low frequency. With its limitation to ~930 kyr, our present record is definitely too short to check these hypotheses, and future work is needed toward answering this question. This will also help to understand whether the reduced dust flux during the MPT is a local signal or reflects a regional or global climate pattern.

[38] Comparing the dust flux records (Figure 5) with the calcium carbonate record (Figure 2) reveals a strong similarity. The lower dust levels during the MPT correlate with a period of high calcium carbonate contents (Figure 2) indicative of exceptionally good preservation. Also, both records show a relatively stable signal over the period of the MPT, in comparison to the considerably higher variability during the subsequent glacial/interglacial cycles. Assuming that carbonate preservation is driven by changes in the paleochemistry of the deep Pacific Ocean, i.e., less corrosive waters because of better ventilation of the bottom waters, the systematic correlation between both records indicates a large-scale coordination between the Southern Ocean, where the deep Pacific Ocean is ventilated, and the low-latitude wind fields of the Northern Hemisphere, the probable source region of the dust. This potential long-term teleconnection merits further investigation.

[39] **Acknowledgments.** Joerg Schaefer and Sidney Hemming provided valuable comments on an earlier draft of this paper. We thank Martin Stute for his collaboration and continued support of the lab. We are grateful to A. Mangini, B. Schwarz, C. Strobl, and M. Christl from the ''Radiometric Dating Group'' at the Academy of Sciences Heidelberg who generously provided us with the ^{10}Be data from ODP806 and to Martin Frank for help with the magnetic field corrections for the ^{10}Be data. We thank Marty Fleisher and Yong Lao for the ^{230}Th data. Reviews by Ralf Tiedemann and an anonymous referee are much appreciated. Funding for this research was provided by NSF grant OCE-97-11870. G.W. acknowledges support of the Leopoldina Fellowship from Deutsche Akademie der Naturforscher Leopoldina as well as support from the Comer Science and Education Foundation. Samples were generously provided by the curator at the University of Rhode Island core repository (OCE-9102410). This is LDEO contribution 6805.

References

Anderson, R. F., M. Q. Fleisher, and Y. Lao (2005), Glacial-interglacial variability in the delivery of dust in the central equatorial Pacific Ocean, *Earth Planet. Sci. Lett.*, in press.

Archer, D. E., and E. Maier-Reimer (1994), Effect of deep-sea sedimentary calcite preservation on atmospheric CO_2 concentration, *Nature*, *367*, 260–264.

Arrhenius, G. O. S. (1952), Sediment cores from the east Pacific, in *Report of the Swedish Deep Sea Expeditions, 1947–1948*, pp. 1–228, Elander, Göteborg, Sweden.

Banakar, V. K., G. Parthiban, J. N. Pattan, and P. Jauhari (1998), Chemistry of surface sediments along a north-south transect across the equator in the central Indian Basin: An assessment of biogenic and detrital influences on elemental burial on the seafloor, *Chem. Geol.*, *147*, 217–232.

Bishop, J. K. B. (1988), The barite-opal-organic carbon association in oceanic particulate matter, *Nature*, *332*, 341–343.

Bopp, L., K. E. Kohfeld, C. Le Quere, and O. Aumont (2003), Dust impact on marine biota and atmospheric CO_2 during glacial periods, *Paleoceanography*, *18*(2), 1046, doi:10.1029/2002PA000810.

Broecker, W. S., and G. M. Henderson (1998), The sequence of events surrounding Termination II and their implications for the cause of glacial-interglacial CO_2 changes, *Paleoceanography*, *13*, 352–364.

Brook, E. J., M. D. Kurz, J. Curtice, and S. Cowburn (2000), Accretion of interplanetary dust in polar ice, *Geophys. Res. Lett.*, *27*, 3145–3148.

Chuey, J. M., D. K. Rea, and N. G. Pisias (1987), Late Pleistocene paleoclimatology of the central equatorial Pacific: A quantitative record of eolian and carbonate deposition, *Quat. Res.*, *28*, 323–349.

Clarke, W. B., W. J. Jenkins, and Z. Top (1976), Determination of tritium by mass spectrometric measurement of ^{3}He, *Int. J. Appl. Radiat. Isot.*, *27*, 515–522.

Dean, W. E., J. V. Gardner, and D. A. Piper (1997), Inorganic geochemical indicators of glacial-interglacial changes in productivity and anoxia on the California continental margin, *Geochim. Cosmochim. Acta*, *61*, 4507–4518.

Delaney, M. L. (1998), Phosphorus accumulation in marine sediments and the oceanic phosphorus cycle, *Global Biogeochem. Cycles*, *12*, 563–572.

Dymond, J., E. Suess, and M. Lyle (1992), Barium in deep-sea sediment: A geochemical proxy for productivity, *Paleoceanography*, *7*, 163–181.

Dymond, J., R. Collier, J. McManus, S. Honjo, and S. Manganini (1997), Can the aluminum and titanium contents of ocean sediments be used to determine the paleoproductivity of the oceans?, *Paleoceanography*, *12*, 586–593.

Farley, K. A. (1995), Cenozoic variations in the flux of interplanetary dust recorded by ^{3}He in a deep-sea sediment, *Nature*, *376*, 153–156.

Farley, K. A. (2001), Extraterrestrial helium in seafloor sediments: Identification, characteristics, and accretion rate over geological time, in *Accretion of Extraterrestrial Matter Throughout Earth's History*, edited by B. Peucker-Ehrenbrink and B. Schmitz, pp. 179–204, Springer, New York.

Farley, K. A., S. G. Love, and D. B. Patterson (1997), Atmospheric entry heating and helium retentivity of interplanetary dust particles, *Geochim. Cosmochim. Acta*, *61*, 2309–2316.

Farrell, J. W., and W. L. Prell (1989), Climate change and $CaCO_3$ preservation: An 800,000 year bathymetric reconstruction from the central equatorial Pacific Ocean, *Paleoceanography*, *4*, 447–466.

Feely, R. A., R. Wanninkhof, T. Takahashi, and P. Tans (1999), Influence of El Niño on the equatorial Pacific contribution to atmospheric CO_2 accumulation, *Nature*, *398*, 597–601.

Francois, R., S. Honjo, S. J. Manganini, and G. E. Ravizza (1995), Biogenic barium fluxes to the deep sea: Implications for paleoproductivity reconstructions, *Global Biogeochem. Cycles*, *9*, 289–303.

Francois, R., M. Frank, M. Rutgers van der Loeff, and M. P. Bacon (2004), ^{230}Th normalization: An essential tool for interpreting sedimentary fluxes during the late Quaternary, *Paleoceanography*, PA1018, doi:10.1029/2003PA000939.

Frank, M., R. Gersonde, M. Rutgers van der Loeff, G. Bohrmann, C. C. Nuernberg, P. W. Kubik, M. Suter, and A. Mangini (2000), Similar glacial and interglacial export productivity in the Atlantic sector of the Southern Ocean: Multiproxy evidence and implications for glacial atmospheric CO_2, *Paleoceanography*, *15*, 642–658.

Froelich, P., M. L. Bender, N. A. Luedtke, G. R. Heath, and T. De Vries (1982), The marine phosphorous cycle, *Am. J. Sci.*, *282*, 474–511.

Goldberg, E. D., and G. O. S. Arrhenius (1958), Chemistry of Pacific pelagic sediments, *Geochim. Cosmochim. Acta*, *13*, 153–212.

Guyodo, Y., and J.-P. Valet (1999), Global changes in intensity of the Earth's magnetic field during the past 800 kyr, *Nature*, *399*, 249–252.

Harrison, S. P., K. E. Kohfeld, C. Roelandt, and T. Claquin (2001), The role of dust in climate changes today, at the last glacial maximum and in the future, *Earth Sci. Rev.*, *54*, 43–80.

Knowlton, C. W. (1998), Productivity controls on carbonate cycles in the central equatorial Pacific Ocean during the late Pleistocene, M.S. thesis, Univ. of R.I., Narrangansett.

Kohfeld, K. E., and S. P. Harrison (2001), DIRTMAP: The geological record of dust, *Earth Sci. Rev.*, *54*, 81–114.

Kohfeld, K. E., C. L. Quere, S. P. Harrison, and R. F. Anderson (2005), Role of marine biology in glacial-interglacial CO_2 cycles, *Science*, *308*, 74–78.

Kryc, K. A., R. W. Murray, and D. W. Murray (2003), Al-to-oxide and Ti-to-organic linkages in biogenic sediment: Relationships to paleo-export production and bulk Al/Ti, *Earth Planet. Sci. Lett.*, *211*, 125–141.

Latimer, J. C., and G. M. Filippelli (2002), Phosphorus geochemistry and export production across the polar front zone in the southeastern Atlantic Ocean, *Geochim. Cosmochim. Acta*, *66*, A434.

Marcantonio, F., N. Kumar, M. Stute, R. F. Anderson, M. A. Seidl, P. Schlosser, and A. Mix (1995), A comparative study of accumulation rates derived by He and Th isotope analysis of marine sediments, *Earth Planet. Sci. Lett.*, *133*, 549–555.

Marcantonio, F., R. F. Anderson, M. Stute, N. Kumar, P. Schlosser, and A. Mix (1996), Extraterrestrial ^{3}He as a tracer of marine sediment transport and accumulation, *Nature*, *383*, 705–707.

Marcantonio, F., R. F. Anderson, S. Higgins, M. Stute, P. Schlosser, and P. Kubik (2001), Sediment focusing in the central equatorial Pacific Ocean, *Paleoceanography*, *16*, 260–267.

Masarik, J., and J. Beer (1999), Simulation of particle fluxes and cosmogenic nuclide production in the Earth's atmosphere, *J. Geophys. Res.*, *104*, 12,099–12,111.

Murray, R. W., and M. Leinen (1993), Chemical transport to the seafloor of the equatorial Pacific Ocean across a latitudinal transect at 135W: Tracking sedimentary major, trace, and rare earth element fluxes at the equator and the Intertropical Convergence Zone, *Geochim. Cosmochim. Acta*, *57*, 4141–4163.

Murray, R. W., and M. Leinen (1996), Scavenged excess Al and its relationship to bulk Ti in biogenic sediment from the central equatorial Pacific Ocean, *Geochim. Cosmochim. Acta*, *60*, 3869–3878.

Murray, R. W., M. Leinen, and A. R. Isern (1993), Biogenic flux of Al to sediment in the central equatorial Pacific Ocean: Evidence for increased productivity during glacial periods, *Paleoceanography*, *8*, 651–670.

Murray, R. W., M. Leinen, D. W. Murray, A. C. Mix, and C. W. Knowlton (1995), Terrigenous Fe input and biogenic sedimentation in the glacial and interglacial equatorial Pacific Ocean, *Global Biogeochem. Cycles*, *9*, 667–684.

Murray, R. W., C. Knowlton, M. Leinen, A. C. Mix, and C. H. Polsky (2000), Export productivity and carbonate dissolution in the central equatorial Pacific Ocean over the past 1 Myr, *Paleoceanography*, *15*, 570–592.

Nier, A. O., and D. J. Schlutter (1992), Extraction of helium from individual interplanetary dust particles by step-heating, *Meteoritics*, *27*, 166–173.

Nürnberg, C. C., G. Bohrmann, and M. Schlüter (1997), Barium accumulation in the Atlantic sector of the Southern Ocean: Results from 190,000-year record, *Paleoceanography*, *12*, 594–603.

Ozima, M., and F. Podosek (1983), *Noble Gas Geochemistry*, Cambridge Univ. Press, New York.

Patterson, D. B., and K. A. Farley (1998), Extraterrestrial ^{3}He in seafloor sediments: Evidence for correlated 100 kyr periodicity in the accretion rate of interplanetary dust, orbital parameters, and Quaternary climate, *Geochim. Cosmochim. Acta*, *62*, 3669–3682.

Patterson, D. B., K. A. Farley, and M. D. Norman (1999), ^{4}He as a tracer of continental dust: A 1.9 million year record of aeolian flux to the west equatorial Pacific Ocean, *Geochim. Cosmochim. Acta*, *63*, 615–625.

Paytan, A., M. Kastner, and F. P. Chavez (1996), Glacial to interglacial fluctuations in productivity in the equatorial Pacific as indicated by marine barite, *Science*, *274*, 1355–1357.

Raymo, M. E., D. W. Oppo, and W. Curry (1997), The mid-Pleistocene climate transition: A deep sea carbon isotopic perspective, *Paleoceanography*, *12*, 546–549.

Rea, D. K. (1990), Aspects of atmospheric circulation: The Late Pleistocene (0–950,000 yr) record of eolian deposition in the Pacific Ocean, *Palaeogeogr. Palaeoclimatol. Palaeoecol.*, *78*, 217–227.

Rea, D. K. (1994), The paleoclimatic record provided by eolian deposition in the deep sea: The geologic history of wind, *Rev. Geophys.*, *32*, 159–195.

Schwarz, B., A. Mangini, and M. Segl (1996), Geochemistry of a piston core from Ontong Java Plateau (western equatorial Pacific): Evidence for sediment redistribution and changes in paleoproductivity, *Geol. Rundsch.*, *85*, 536–545.

Takahashi, T., R. A. Feely, R. F. Weiss, R. H. Wanninkhof, D. W. Chipman, S. C. Sutherland, and T. T. Takahashi (1997), Global air-sea flux of CO_2: An estimate based on measurements of sea-air pCO_2 difference, *Proc. Natl. Acad. Sci. U. S. A.*, *94*, 8292–8299.

Takahashi, T., et al. (2002), Global sea-air CO_2 flux based on climatological surface ocean pCO_2, and seasonal biological and temperature effects, *Deep Sea Res., Part II*, *49*, 1601–1622.

Valet, J.-P., and L. Meynadier (1993), Geomagnetic-field intensity and reversals during the past 4 million years, *Nature*, *366*, 234–238.

Winckler, G., R. F. Anderson, M. Stute, and P. Schlosser (2004), Does interplanetary dust control 100 kyr cycles?, *Quat. Sci. Rev.*, *23*, 1873–1878.

R. F. Anderson, P. Schlosser, and G. Winckler, Lamont-Doherty Earth Observatory of Columbia University, 61 Route 9W, Palisades, NY 10964, USA. (winckler@ldeo.columbia.edu)